

Gradient Arrays for High Performance Multiple Region MRI

D. L. Parker¹, J. R. Hadley¹

¹Radiology, University of Utah, Salt Lake City, UT, United States

Introduction In MRI, there is a trade-off between the gradient field-of-view (GFOV), performance (gradient amplitude and slew rate) and nerve stimulation threshold. Increased performance has generally required reduced GFOV to avoid nerve stimulation¹⁻³. Although reduced GFOV is consistent with the general trend towards smaller MRI scanners, there are many applications where large region imaging is important. We have investigated the use of overlapping multiple region gradient arrays to allow imaging over an extended GFOV with increased gradient performance and reduced total magnetic field excursion. Although multiple region gradients were first mentioned in a patent by Oppelt,⁴ this is the first work to investigate the basic designs of such gradient systems, and to predict the relative performance parameters. **Z-gradient:** The simplest Z-gradient set is the Maxwell Pair created by two current dipoles as illustrated in Fig. 1. The arrows indicate directions of the loop dipole. The number and positions of the wires in each dipole are specified to approximate the desired performance. **Maxwell Arrays:** By dividing the GFOV into multiple regions, the same gradient performance can be achieved while reducing the excursion of the magnetic field. In general, it is possible to achieve high gradient performance over GFOV's of arbitrary length by using gradient arrays with the desired numbers of regions. **Transverse-Gradient Array:** The transverse gradient, typically formed by fingerprint wire patterns around the cylinder, can also be converted into arrays by adding more patterns as shown in Fig. 2. The arrows indicate current dipole directions for the double region gradient.

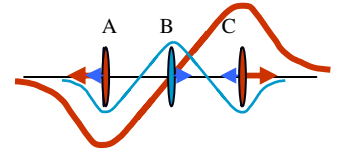


Figure 1: Maxwell Pair (red, using coils A and C) vs. Maxwell Triplet (blue, using coils A, B, and C)

Methods Following the discussion of Tomasi⁵, stream functions were used to specify the current distributions for both longitudinal and transverse unshielded gradient coils. Generalization to include shields is straightforward. Simulated annealing (SA) was used with a reasonable figure of merit (FOM) to obtain a large number of samples of gradient performance factors in the solution space. The set of solutions was reviewed and trade-offs between the solutions driven by the chosen FOM were evaluated.⁶ For the Z-

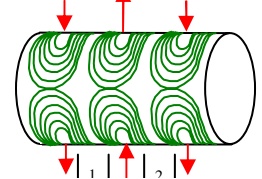


Figure 2: Double region transverse-gradient array windings

array: $fom = \sqrt{L} \sigma_{ms} / \eta$ where $\sigma_{ms} = \sqrt{\frac{1}{V} \int_{GFOV} (B_z(\vec{r}) - zG_z)^2 dx dy dz}$, $G_z = \int_{GFOV} z B_z(\vec{r}) dx dy dz / \int_{GFOV} z^2 dx dy dz$, η is

the gradient per unit current, and V is the volume of the GFOV. For the transverse gradient array, a large variability was observed in the total magnetic field external to the imaging volume. To create solutions that constrained this variability, it became useful to explore solutions that also minimized the total field external to the imaging regions of interest, but potentially within the bodies of large subjects. In this case, we used: $fom = \sqrt{L} \sigma_{ms} B_{max}(\rho = 5R/6) / \eta^2$, where $B_{max}(\rho)$ is the maximum of the total magnetic field on a cylinder of radius, ρ . Although the potential for nerve stimulation is difficult to assess, it is assumed that this potential increases as the gradient magnetic field increases. In general the magnetic field created by the gradients increases towards the gradient windings. To provide a qualitative comparison of the potential for nerve stimulation, we chose to calculate the maximum of the total magnetic field at a distance of 5/6 of the winding radius, $B_{max5/6}$. This field is outside of the imaging volume, given that the radius of the imaging volume was selected to be 3/4 of the winding radius, R , but may still lie within the subject being imaged.

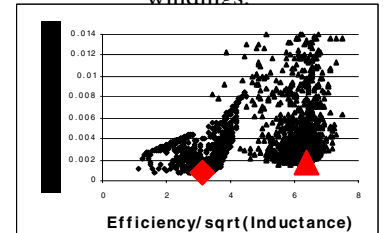


Figure 3: Example SA results for single and double region Z-grad coil, FOV_z = 90, FOV_x = 45, length/radius = 150/30cm. Realizations of single and double region coils produce point clouds at the left and right (resp) of plot. The selected operating point is indicated by the large symbol.

Results SA was used to create families of stream functions and corresponding gradient wiring patterns for a variety of imaging volumes. From the range of results, the stream function that gave the best compromise in performance parameters was selected. Using a conductor cylinder of $R=30$ cm, gradients were designed to cover cylindrical imaging volumes of $FOV_z(\text{cm})/FOV_x(\text{cm}) = 90/22.5, 60/22.5, 51/22.5,$ and $51/11$. (potentially useful for small

animals and proof of principle). Two sets of gradient wiring dimensions, GFOV, and performance parameters from the selected stream functions are summarized in Table 1. FOV_z/FOV_x are the length (z) and radius (x) of GFOV, the cylinder over which the homogeneity is measured. For the single region coil, the inhomogeneity, defined as the RMS deviation of the predicted field from the desired field, is computed over the entire cylinder volume. For the double region coil, the homogeneity is computed over the desired smaller volume (segment length is $FOV_z/3$). Z and R are the dimensions of the cylinder over which the coil windings are placed. In every case, η of the double region coil is higher than that of the single region coil for the same inductance and the maximum gradient magnetic field is much less.

Discussion/Conclusions We have demonstrated that gradient arrays can be designed to provide multiple region imaging with increased relative efficiency and reduced magnetic fields compared to single region arrays that cover comparable imaging volumes. The improvement in gradient performance is greatest when the aspect ratio (FOV_z/FOV_x) is large, but improvement still exists when designing for shorter systems such as might be found in existing imaging magnets.

Acknowledgments We thank Brian Rutt and Blaine Chronik of the University of Western Ontario. Supported by R21 EB004803 and Siemens Medical Solutions.

References

1. Imrich W, Schmitt F. Magnetostimulation in MRI. *Magn Reson Med.* May 1995;33(5):619-623.
2. Chronik BA, Rutt BK. A comparison between human magnetostimulation thresholds in whole-body and head/neck gradient coils. *Magn Reson Med.* Aug 2001;46(2):386-394.
3. Chronik BA, Rutt BK. Simple linear formulation for magnetostimulation specific to MRI gradient coils. *Magn Reson Med.* May 2001;45(5):916-919.
4. Oppelt A, inventor; Siemens Aktiengesellschaft, Munich, Germany, assignee. Nuclear Magnetic Resonance tomography device and method for its operation. US patent US 6,255,821 B1. July 3, 2001, 2001.
5. Tomasi D. Stream function optimization for gradient coil design. *Magn Reson Med.* Mar 2001;45(3):505-512.
6. Du YP, Parker DL. Studies on the performance of circular and elliptical Z-gradient coils using a simulated annealing algorithm. *Magn Reson Imaging.* 1997;15(2):255-262.

Table 1. Some example comparative coil designs. All gradients are designed assuming inductance, $L=1200\mu\text{H}$.

Coil type	FOV _z /x (cm)	Z/R (cm)	η mT/mA	RMS ($\mu\text{T/A}$)	$B_{0_{max5/6}}$ r=5a/6
Z(1)	90/22.5	150/30	109	0.40	29.4
Z(2)	90/22.5	150/30	224	2.00	12.0
X(1)	90/22.5	150/30	83.5	0.17	80.9
X(2)	90/22.5	150/30	150	0.18	46.5
Z(1)	60/22.5	120/30	155	0.65	20.4
Z(2)	60/22.5	120/30	311	4.13	9.53
X(1)	60/22.5	140/30	124	0.56	43.4
X(2)	60/22.5	140/30	218	2.60	26.9